

# Synthetic nucleic acid secondary structures containing the four stereoisomers of 1,4-bis(thymine-1-yl)butane-2,3-diol†

Mikkel S. Christensen,<sup>a,b</sup> Andrew D. Bond<sup>b</sup> and Poul Nielsen<sup>\*a,b</sup>

Received 10th September 2007, Accepted 17th October 2007

First published as an Advance Article on the web 7th November 2007

DOI: 10.1039/b713888a

The four stereoisomers of the double-headed acyclic nucleoside 1,4-bis(thymine-1-yl)butane-2,3-diol were incorporated in the central position of four 13-mer oligonucleotides. The phosphoramidite building blocks were synthesized in four or six steps from either D- or L-2,3-O-isopropylidene-threitol. Two epimeric and fully deprotected double-headed nucleosides were analyzed by X-ray crystallography. The incorporation into oligonucleotides was hampered by steric hindrance and formation of a cyclic phosphate. The use of pyridinium chloride as the activator and a kinetic analysis based on <sup>31</sup>P NMR of the coupling and detritylation processes led to improved yields of the oligonucleotides. In comparison with the (*S*)-GNA monomer, one of the four stereoisomers was found to show a similar destabilization of a DNA duplex, indicating that the additional base can be introduced without a thermal penalty. Another stereoisomer was found to induce a thermal stabilization of a DNA:RNA three-way junction. Thus, the stereochemistry of this acyclic double-headed nucleoside motif is important, indicating potential for the design of artificial nucleic acid secondary structures.

## Introduction

Synthetic nucleic acid chemistry has been predominantly motivated by the potential of selective nucleic acid based therapeutics using gene silencing approaches.<sup>1,2</sup> Nevertheless, new perspectives appear within nucleic acid nanobiotechnology and nanoscale engineering.<sup>3–5</sup> The synthetic design is based on the predictable Watson–Crick base pairing capacity of nucleic acids. Simple duplexes built with canonical base pairing, however, span quite a restricted set of possible structure types. Nucleic acid secondary structures are envisioned to be among the structural elements that may form the foundation of bottom-up constructs within nanotechnology.<sup>5</sup> Thus, within synthetic nucleic acid chemistry, there has been a drive to expand the structural diversity by mimicking natural secondary structures other than duplexes, such as bulges and three-way junctions, through application of synthetic nucleoside analogs.<sup>6,7</sup> In this line of research, non-conventional nucleosides bearing two nucleobases (called double-headed nucleosides) have been synthesized, to give nucleic acids that provide an extra recognition possibility for either interstrand or intrastrand communication.<sup>8–11</sup>

Nucleosides based on the natural 2'-deoxyribonucleoside structure but with an additional nucleobase attached in different

positions have been studied (Fig. 1). Thus, we introduced the two double-headed nucleosides **1** and **2** with the additional thymine positioned in either the 2'- or the 5'-position,<sup>9,11</sup> whereas Herdewijn and co-workers introduced **3** with either an additional thymine or an adenine in the 4'-position.<sup>10</sup> Furthermore, a simpler acyclic double-headed nucleoside **4** has been studied.<sup>8</sup> In our studies, oligodeoxynucleotides (ODNs) containing **1** or **2** were used to form bulged and three-way junction structures. In other studies, we have approached these structures with more complicated cyclic dinucleotides,<sup>12,13</sup> but the simpler constructs were synthetically more appealing and, in fact, more promising. Thus, **1** incorporated in the branching point of a nucleic acid three-way junction increased the thermal stability of this significantly.<sup>9</sup> The double-headed nucleosides **3** and **4** were mainly studied for developing interstrand communication between complementary nucleic acid sequences through base–base H-bond interaction on the duplex surface.<sup>8,10</sup> On the other hand, a strong base–base stacking interaction in the minor groove was found for two complementary ODNs containing **2** in a zipper motif.<sup>11</sup>

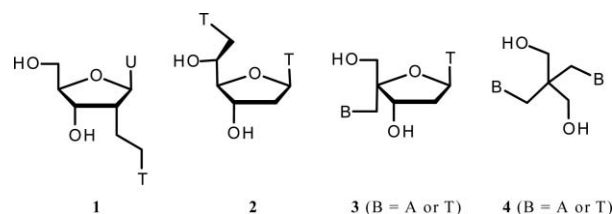


Fig. 1 Double-headed nucleosides. U = uracil-1-yl, T = thymine-1-yl, A = adenine-9-yl.

In this paper we wish to report our efforts towards simpler acyclic double-headed nucleoside building blocks mimicking the very simple (*S*)-GNA (glycerol nucleic acid) structure (Fig. 2) reported earlier by us<sup>14</sup> and others,<sup>15,16</sup> and elaborated recently by

<sup>a</sup>Nucleic Acid Center, University of Southern Denmark, 5230, Odense M, Denmark

<sup>b</sup>Department of Physics and Chemistry, University of Southern Denmark, 5230, Odense M, Denmark. E-mail: pon@ifk.sdu.dk; Fax: +45 66158780; Tel: +45 65502565

† Electronic supplementary information (ESI) available: Data supporting the kinetic experiments on the phosphoramidite coupling sequences as well as <sup>1</sup>H NMR analysis for **13** and **14**; crystal structure data. See DOI: 10.1039/b713888a

‡ The Nucleic Acid Center is funded by the Danish National Research Foundation for studies on nucleic acid chemical biology.

§ The Nucleic Acid Center is funded by the Danish National Research Foundation for studies on nucleic acid chemical biology.

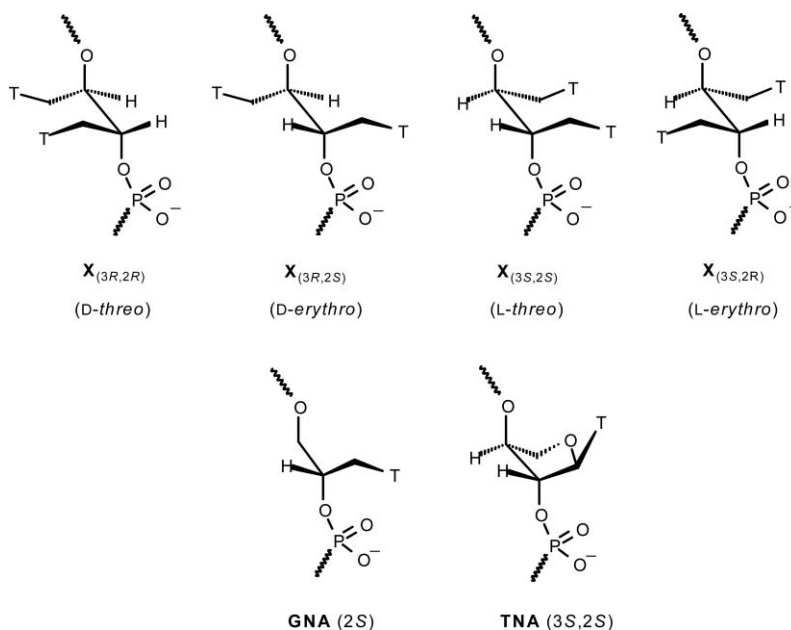


**Fig. 2** Incorporation of the four stereoisomers of 1,4-bis(thymine-1-yl)butane-2,3-diol into ODNs compared to GNA and TNA. T = thymine-1-yl.

Meggens *et al.* to fully modified sequences forming a surprisingly stable antiparallel base pairing system.<sup>17,18</sup> This system, which can be regarded as an acyclic analog of the TNA (threitol nucleic acid) reported by Eshenmoser and co-workers<sup>19</sup> (Fig. 2), has also been shown to form stable cross-pairing with RNA. We decided to elaborate the simple glycerol skeleton to an erythrol/threitol system with two thymines, preparing and incorporating the four different stereoisomers of 1,4-bis(thymine-1-yl)butane-2,3-diol into ODNs (X, Fig. 2) in order to study their effect on DNA and RNA secondary structures. Due to the non-restricted rotation around the C2'–C3' bond, the glycols are envisioned to conform better to these non-canonical structures than natural nucleosides or, possibly, better than the double-headed nucleosides with the natural 2'-deoxyribofuranose skeleton.

## Results and discussion

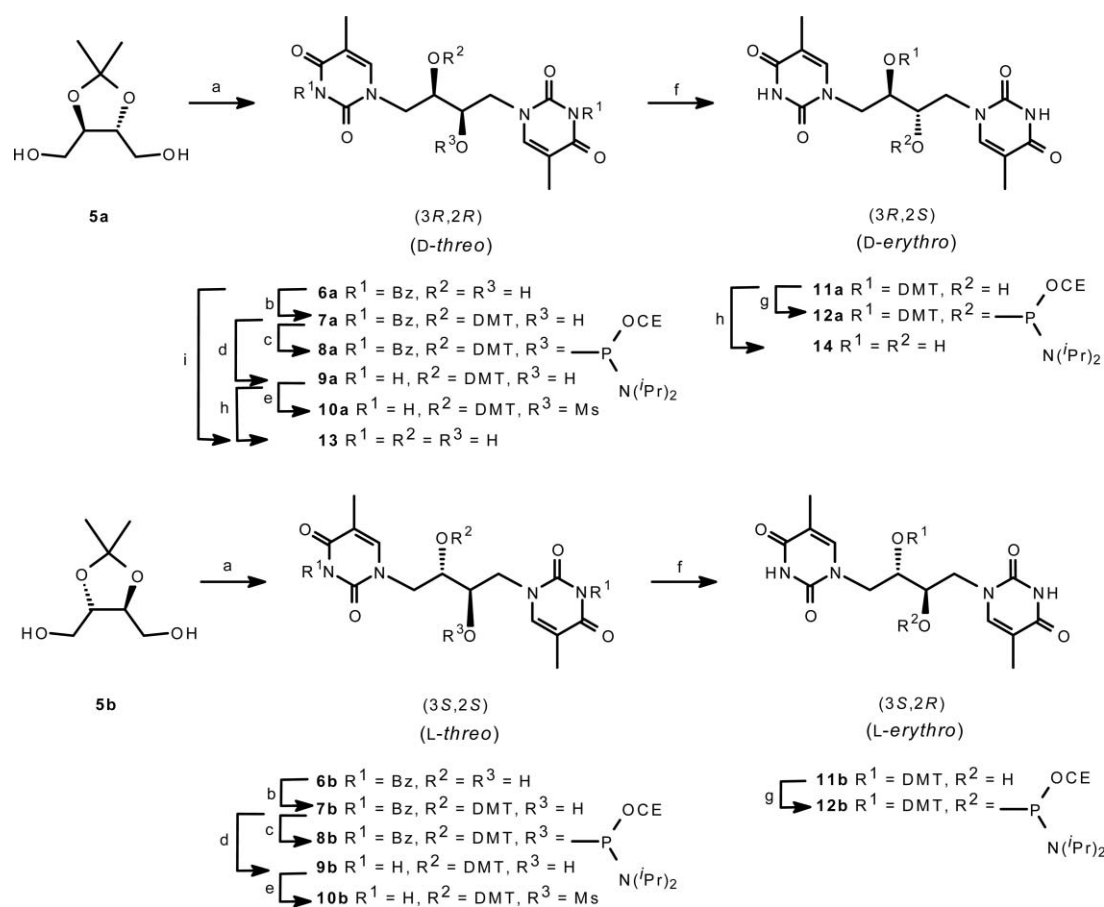
### Chemical synthesis

The four diastereoisomeric double-headed phosphoramidite building blocks were synthesised from the two commercially available enantiopure compounds D- and L-2,3-*O*-isopropylidene threitol, **5a** and **5b**, respectively (Scheme 1). A Mitsunobu reaction<sup>20</sup> with N3-benzoylated thymine<sup>21,22</sup> furnished the regioselective N1-alkylation of thymine. After chromatography, the compounds were taken directly to the next step and hydrolysed by a standard protocol to give the double-headed nucleosides **6a** and **6b** in a yield of 50 and 36% over the two steps, somewhat hampered by extensive chromatography well known for the Mitsunobu reaction.<sup>21</sup> The polarity sense of the nucleosides was fixed by protecting one of the symmetry-equivalent hydroxy groups with a DMT group. Hence, selective DMT-protection by treatment with excess DMTCl in anhydrous pyridine afforded the two enantiopure compounds **7a** and **7b** constituting a divergence point between the *threo*- and *erythro*-configured stereoisomers. With the orientation set by the DMT protection, the projected

*threo*-configured phosphoramidites **8a** and **8b** were immediately obtained after isolation of the DMT-protected glycols in 74 and 77% yield followed by a standard phosphitylation in 64 and 39% yield. To render an *erythro*-configuration, an inversion at the C2' alcohol was required prior to phosphitylation. An approach involving the participation of the neighboring thymine was envisioned. To facilitate the enolic tautomer of the thymine base, compounds **7a** and **7b** were debenzoylated, and the compounds **9a** and **9b** were prepared in overall yields of 11 and 18% based on the starting materials **5a** and **5b**. A leaving group was introduced by mesylation in 41 and 50% yield to give **10a** and **10b**, and the configuration was subsequently inverted by treatment with aqueous NaOH in ethanol.<sup>23</sup> The reaction presumably occurs *via* the anticipated intermediary O2-anhydro compound, which is subsequently hydrolysed. By analogy, Holy isolated the O2-anhydro compound obtained from the corresponding GNA-monomer 3-dimethoxytrityloxy-2-mesyloxy-1-(thymine-1-yl)propane treated with Et<sub>3</sub>N under anhydrous conditions.<sup>16</sup> The erythritols **11a** and **11b** were obtained in 84 and 88% yield and finally phosphitylated to give the amidites **12a** and **12b** in 69 and 64% yield.

### X-Ray crystallography, NMR spectroscopy and molecular modelling

Confirmation of the C2' inversion was made possible by crystallization of the fully deprotected compounds **13** and **14** obtained from acidic hydrolysis on the analytical scale of compounds **9a** and **11a**, respectively. Compound **13** has also been prepared directly from **6a**. Thus, the *D-threo*- and the *meso*-1,4-bis(thymine-1-yl)-2,3-butanediol, **13** and **14**, respectively, were crystallized from a DMSO–water system to give the structures shown in Fig. 3. Both molecules were found to form an extended H-bonded network in the crystalline state. Both molecules assume the expected conformation based on *gauche* interactions between the electronegative substituents around the C1'–C2' bond. On the



**Scheme 1** Reagents and conditions: (a) i. 3-*N*-benzoylthymine,  $\text{Ph}_3\text{P}$ , DEAD, THF; ii. TFA– $\text{H}_2\text{O}$  (3 : 1) (**6a** 50% and **6b** 36%); (b) DMTCl, pyr (**7a** 74% and **7b** 77%); (c) CEOPCIN(*i*-Pr) $_2$ , DIPEA,  $\text{CH}_2\text{Cl}_2$  (**8a** 64% and **8b** 39%); (d) aq. NaOH, dioxane (**9a** 11% from **5a** and **9b** 18% from **5b**); (e) MsCl, Pyr (**10a** 41% and **10b** 50%); (f) aq. NaOH, EtOH (**11a** 84% and **11b** 88%); (g) CEOPCIN(*i*-Pr) $_2$ , DIPEA, DCM (**12a** 69% and **12b** 64%); (h) DCA– $\text{SiO}_2$ , DCM; (j) 80% aq. AcOH (42% from **5a**). CE = 2-Cyanoethyl. DMT = 4,4'-Dimethoxytrityl.

other hand, only the *threo*-configured isomer **13** conforms to this theory for the C2'–C3' bond as well, while the *erythro*-configured **14** assumes an antiperiplanar conformation for all its substituents. This could indicate that the *anti* relationship for the methylene (thymine) groups in this case is more important than the *gauche* interactions for the electronegative groups.

Conformational analysis based on the  $^1\text{H}$  NMR coupling constants from **13** in  $\text{DMSO-}d_6$  also indicates an average *gauche* (+) conformation around the C1'–C2' bond ( $J = 2$  Hz, 9 Hz and 13 Hz) (see ESI-Fig. 1). For **14**, similar coupling constants also indicated this conformation ( $J \sim 0$  Hz, 8 Hz and 13 Hz). The alternative *gauche* (–) conformation with a similar coupling constant pattern seems less likely because of the unfavorable steric overlap from the butane moiety and the pyrimidine. It was not possible to discern the conformation around the C2'–C3' bond from coupling constants. Nevertheless, the conformation around the C1'–C2' bond discourages the possibility that the thymine bases stack intramolecularly in solution; a conformation that potentially could later impede its ability to fit properly into a duplex environment.

In order to investigate how well the structures adapt to a B-type DNA environment, models with the two isomers  $\text{X}_{(3S,2S)}$  (*L-threo*) and  $\text{X}_{(3R,2S)}$  (*D-erythro*) were investigated with a 0.5 ns MD-simulation (Fig. 4). Initially, the monomers in the conformations

obtained from the X-ray analysis were used as starting points. Due to the 2(*S*)-configuration, the particular two isomers mimic the (*S*)-GNA carbon framework; moreover, the  $\text{X}_{(3R,2S)}$  monomer assumes a conformation that resembles the quasi-2',3'-*trans*-diaxial backbone of TNA with its 2',3'-antiperiplanar backbone. The models in Fig. 4a and b indicate that the crystal state conformations are accommodated well in a B-DNA duplex with the extra base placed on the outside of the helix. Rotation around the C1'–C2' bond is the only significant adaptation required to maintain base pairing. However, the P–P internucleotide distance fluctuates around 4.9 Å for  $\text{X}_{(3S,2S)}$  and 5.9 Å for  $\text{X}_{(3R,2S)}$  compared with 6.5 Å for the normal backbone. The short distance of 4.9 Å may be an incitement for the *threo*-configured  $\text{X}_{(3S,2S)}$  to shift the conformation to a 2',3'-antiperiplanar backbone. Indeed, a similar MD-simulation with  $\text{X}_{(3S,2S)}$  in this conformation (Fig. 4c) and another with the C3'–C4' bond also assuming an antiperiplanar conformation (Fig. 4d) give longer P–P internucleotide distances, around 5.3 Å and 5.9 Å, respectively.

### Synthesis of oligodeoxynucleotides

Table 1 presents the oligodeoxynucleotides (ODNs) prepared in this study. To investigate the effect of the four stereoisomeric double-headed nucleosides on DNA and RNA secondary

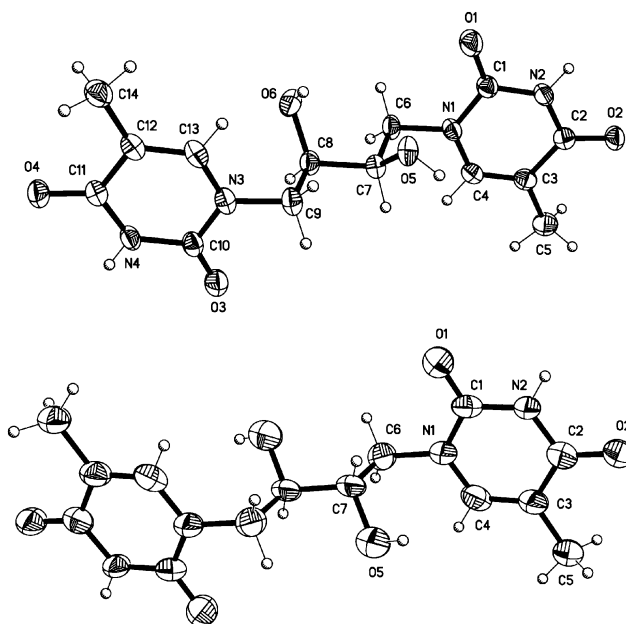


**Fig. 3** X-Ray crystal structures of the deprotected double-headed nucleosides **13** (top) and **14** (bottom). Displacement ellipsoids are shown at the 50% probability level for non-H atoms. In the *meso*-isomer **14**, unlabelled atoms are related to labelled atoms by a crystallographic center of inversion.

**Table 1** Oligodeoxynucleotides prepared for this study

	ODN sequences <sup>a</sup>	MW (found/calc.) <sup>b</sup>
Ref.	5'-GCTCACTCTCCCA	—
<b>ON1</b>	5'-GCTCACX <sub>(3,R,2,R)</sub> CTCCCA	3925.7/3925.1
<b>ON2</b>	5'-GCTCACX <sub>(3,R,2,S)</sub> CTCCCA	3925.7/3926.1
<b>ON3</b>	5'-GTCACX <sub>(3,S,2,S)</sub> CTCCCA	3925.7/3925.6
<b>ON4</b>	5'-GTCACX <sub>(3,S,2,R)</sub> CTCCCA	3925.7/3926.1
<b>ON5</b>	5'-GCTCACT <sub>(2,S)</sub> CTCCCA	3787.7/3788.5
<b>ON6</b>	5'-GTCACECTCCCA	3649.7/3645.9

<sup>a</sup> X refers to the incorporation of **8a**, **12a**, **8b** and **12b**, respectively. T refers to the incorporation of the GNA–T phosphoramidite and E to the ethylene glycol phosphoramidite. <sup>b</sup> MALDI-MS data obtained in negative mode.

structures, four ODNs incorporating any of the four building blocks at the target site were synthesized (**ON1–ON4**). An ODN that contains GNA–T allowing for a single base pairing was included in the study (**ON5**) to investigate the effect of the extra (thymine-1-yl)methyl moiety. Furthermore, an ODN containing just an ethylene glycol linker providing no possibility for base pairing was included (**ON6**).

The six ODNs were synthesised on an automated DNA synthesiser employing phosphoramidite chemistry and standard coupling procedures with 4,5-dicyanoimidazole as the activator except for the non-conventional nucleosides, for which we used pyridinium chloride (pyrHCl) as the activator. This activator has been shown to give good coupling with ribofuranosyl phosphoramidites containing bulky protecting groups on the 2'-hydroxyl group,<sup>24</sup> and in a preliminary experiment, 1*H*-tetrazole proved inefficient (see ESI-Fig. 2). With pyrHCl as activator, the incorporation of X = **8a** into the short model ODN-sequence 5'-TTXTT was achieved with 47–58% efficiency with pyrHCl compared to 8–9% for 1*H*-tetrazole. For comparison, the synthesis of the

corresponding  $n - 1$  oligomer 5'-TTTT was also performed. Yield assessment was based on analytical ion chromatography (IC) after spiking and correcting the extinction coefficient by the 4 : 6 ratio of thymine bases (see ESI-Fig. 3). Mass analysis of the product indicated that the major byproducts were  $n - 1$  oligomers missing thymidines [M – 304] for both sequences. There was no detection of an [M – 400] peak corresponding to an oligomer missing the modified nucleoside X. This indicates that elongation must be retarded only after the incorporation of the modification and also rules out insufficient capping. Thus, pyrHCl was found to be the best activator for these amidites, but the overall coupling yield was still around 50%. Thus, when it was attempted to synthesise a tract of four modifications flanked by unmodified 2'-deoxynucleotides, 5'-CGCT-XXXX-TGCG, with X = **8a** using pyrHCl, the isolated yield of the modified oligonucleotide was <2%.

Recently, Zhou *et al.* reported that the elongation step in the phosphoramidite protocol of the 3-amino analogs of GNA was impaired by a cyclization from attack by the nucleophilic amino group on the P(III) level.<sup>25</sup> We studied the similar cyclization as a potential explanation for the low coupling yields of the double-headed phosphoramidites. A <sup>31</sup>P-NMR study of the coupling steps between **8b** and 3'-*O*-*tert*-butyldimethylsilylthymidine did, however, indicate that the steps were fast and quantitative when pyrHCl was employed as activator and *t*-BuOOH as oxidizer, and indicated no formation of cyclic compounds at the P(III) oxidation state during the coupling step (see ESI-Fig. 4). This result is supported by the observed absence of [M – 400] masses for the aforementioned 5'-TTXTT synthesis. Therefore, the coupling with **8b** as the amidite cannot be the reason for poor yields, indicating that the following detritylation or its subsequent coupling with an unmodified phosphoramidite is retarding the elongation.

To investigate the final detritylation reaction, the dinucleotide was resynthesized on a preparative scale and the detritylation step was studied using catalytic amounts (2%) of trichloroacetic acid in CD<sub>2</sub>Cl<sub>2</sub> (Fig. 5). The reaction was very fast ( $t_{1/2}$  < 2 min) as evident by <sup>1</sup>H-NMR, and it can be concluded that the following coupling must be the weak step. However, the same experiment revealed, after longer reaction time, a new set of peaks appearing in the region of the <sup>31</sup>P-NMR around  $\delta = 15$  ppm. This indicates a cyclisation to form a five-membered ring at the P(V) oxidation state<sup>26</sup> (Fig. 5, see also ESI-Fig. 5). The reaction was conducted with both catalytic and stoichiometric amounts of trichloroacetic acid and in both cases found to have a  $t_{1/2} = 2$  h independent of the acid concentration. Thus, while cyclisation reaction is easily avoided in the fast detritylation step, it could represent a plausible mechanism by which elongation is retarded in the subsequent coupling step, if the coupling itself is slower.

The poor coupling was only observed with the *threo*-configured phosphoramidites **8a** and **8b**. The *erythro*-configured amidites **12a** and **12b** along with the GNA–T amidite were coupled using pyrHCl as activator with good yields (>90%).

### Hybridisation studies

The oligonucleotides were annealed with a set of DNA and RNA strands to give various structural motifs at the complementary site of the modification (Table 2). The formation of a duplex with a complementary DNA strand is seen to be destabilised by the replacement of a thymidine with a double-headed nucleoside as

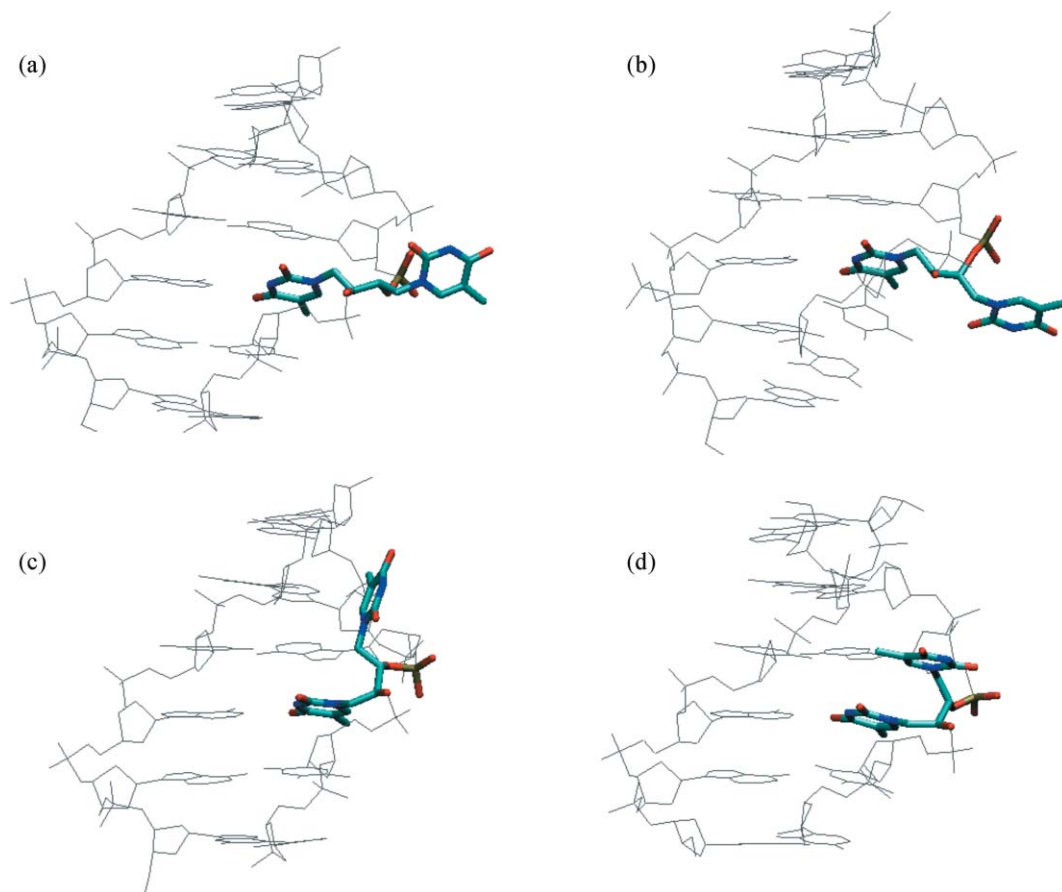


**Fig. 4** Modelling of two double-headed glycol nucleosides (highlighted) placed in a B-DNA environment. The average structures were obtained from the last 50 ps of 500 ps MD-simulations. (a) The *D-erythro*-configured isomer ( $X_{(3R,2S)}$ ) based on the X-ray structure of **14**. (b) The *L-threo*-configured isomer ( $X_{(3S,2S)}$ ) based on the X-ray structure of **13** (inverted stereochemistry) (c) The same *L-threo*-configured isomer with an antiperiplanar conformation of the C2'–C3'-bond. (d) The same *L-threo*-configured isomer with an antiperiplanar conformation of both the C2'–C3' and the C3'–C4' bond.

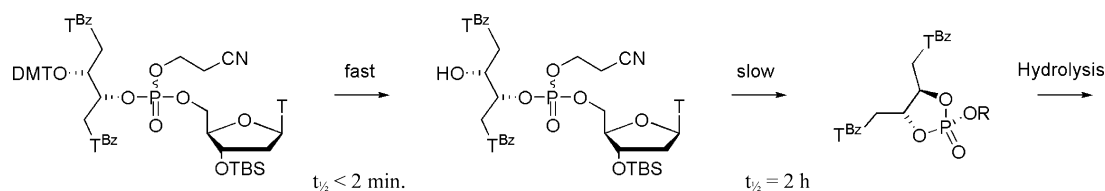


**Fig. 5** Detritylation of the dinucleotide obtained from **8a** with trichloroacetic acid in  $CD_2Cl_2$  at  $T = 24\text{ }^\circ\text{C}$ . The reactions were monitored with  $^1\text{H}$  and  $^{31}\text{P}$  NMR spectroscopy at 200 MHz (see ESI).

evident from the decrease in melting temperatures of  $-10$  to  $-13\text{ }^\circ\text{C}$  (entry 1). On the other hand, the destabilizations are smaller when compared to the insertion of an abasic moiety (**ON6**). Among the four different stereoisomers, the double-headed nucleoside in **ON2** (containing the *D-erythro*-configuration,  $X_{(3R,2S)}$ , see Table 1) does not give any further destabilization, when compared to the GNA-nucleoside in **ON5**. Thus, in the duplex formed with **ON2**, the extra (thymine-1-yl)methyl moiety does not seem to affect the structure significantly. This is in contrast with **ON3**, which has the same C2' configuration but with the C3' configuration inverted (*L-threo*-configuration). The latter duplex is destabilised by about  $2\text{ }^\circ\text{C}$  compared with the former two, indicating that the orientation of the extra (thymine-1-yl)methyl moiety plays a role in the duplex stability.

The model studies (Fig. 4) give some explanation of these results. Considering the structural analogy with TNA–T, for which a crystal structure of its incorporation into a B–DNA duplex is available,<sup>27</sup> the orientation of the methylene linker in **ON3** would point towards the minor groove in an idealised mimic of the O3'–C3'–C2'–O2' antiperiplanar conformation found for TNA–T. Thus, the modelling indicates that the extra base in **ON3** will either align itself with the minor groove (Fig. 4c) or sit perpendicular to the groove (Fig. 4d) depending on the C3'–C4' conformation. In contrast, the extra base in **ON2** seems to be oriented towards the bulk solvent (Fig. 4a). This could indicate that the slightly larger destabilization observed in the **ON3** duplex is partly attributed to a greater perturbation of the minor groove hydration from the presence of the extra thymine base.

**Table 2** Hybridisation data for the prepared ODNs with different DNA- and RNA-complements<sup>a</sup>

Entry	Complements		$T_m/^\circ\text{C}$ Ref.	$\Delta T_m/^\circ\text{C}$					
				ON1	ON2	ON3	ON4	ON5	ON6
1	DNA	3'-dCGAGTGAGAGGGT-5'	52	-13	-10	-12	-12	-10	-16
2	DNA, with mismatch	3'-dCGAGTGTGAGGGT-5'	—	—	-14	—	—	—	—
3	DNA, with mismatch	3'-dCGAGTGGAGGGT-5'	—	—	-10	—	—	—	—
4	DNA, with mismatch	3'-dCGAGTGCAGGGT-5'	—	—	-24	—	—	—	—
5	DNA, A-bulge	3'-dCGAGTGAAGAGGGT-5'	53	-19	-15	-18	-16	ND	-22
6	DNA, AG-bulge	3'-dCGAGTGAGAGGGT-5'	42	-10	-8	-7	-8	ND	-13
7	DNA hairpin (with 10 mM MgCl <sub>2</sub> )	3'-dCGAGTGACGCGT <sub>4</sub> CGCGAGAGGGT-5'	32	-1	-2	-2	-1	ND	-3
8	DNA bulged hairpin (with 10 mM MgCl <sub>2</sub> )	3'-dCGAGTGACCCGCGT <sub>4</sub> CGCGAGAGGGT-5'	33	-6	-5	-6	-5	ND	-7
9	RNA	3'-rCGAGUGAGAGGGU-5'	59	-11	-8	-11	-11	-5	-14
10	RNA, A-bulge	3'-rCGAGUGAAGAGGGU-5'	60	-18	-14	-15	-16	ND	-19
11	RNA, AG-bulge	3'-rCGAGUGAGAGGGU-5'	49	-9	-6	-7	-7	ND	-10
12	RNA hairpin (with 5 mM MgCl <sub>2</sub> ) <sup>b</sup>	3'-rCGAGUGACGCGU <sub>4</sub> CGCGAGAGGGU-5'	39	-3	-2	-3	+2	ND	-4
	(with 10 mM MgCl <sub>2</sub> ) <sup>b</sup>		43	-3	-5	-5	+1	ND	-4
	(with 1 M NaCl) <sup>c</sup>		45	-3	-3	-5	-1	ND	-4
	(with 10 mM MgCl <sub>2</sub> and 1 M NaCl) <sup>b,c</sup>		48	-3	-3	-4	+1	ND	ND
			48	-2	-3	-4	+1	ND	ND

<sup>a</sup> Melting temperatures obtained from the maxima of the first derivatives of the melting curves ( $A_{260}$  vs. temperature) recorded in a medium salt buffer (Na<sub>2</sub>HPO<sub>4</sub> (7.5 mM), NaCl (100 mM), EDTA (0.1 mM), pH 7.0)) using 1.0 μM concentrations of each strand. All  $T_m$  values are given as averages of double determinations.  $\Delta T_m$  values are the differences between the determined  $T_m$  values and the shown  $T_m$  values of the corresponding unmodified reference complexes. ND = Not determined. <sup>b</sup> Obtained by the addition of MgCl<sub>2</sub>. <sup>c</sup> Obtained in a high salt buffer.

A mismatch study (Table 2, entries 2–4) for **ON2** shows large discrimination towards cytidine, but no discrimination towards guanosine and low discrimination towards thymidine. Nevertheless, this indicates that base-pairing is taking place between the double-headed nucleotide and the complementary nucleotide.

Despite the slightly smaller destabilization for **ON2**, the stereochemistry seems in general to be of little importance in the duplex. Insertion of an extra adenosine in the opposite strand (A-bulge) enhances the stereochemical differences and again favors **ON2** over the other sequences (entry 5). However, an overall very large destabilization is evident. In the case of structure **ON1**, the destabilization approaches the result for the abasic analog in **ON6**.

Introducing an additional G bulge between the adenines lowers the relative destabilization (entry 6). In this motif, **ON3** forms the more stable hybrid followed by **ON2** and **ON4**. However, the mismatch study for the ordinary duplex formed by **ON2**, showing no discrimination towards guanosine (entry 3), makes it impossible to discern whether or not an A or a G bulge is actually formed.

The next motif comprises a three-way junction with 10 mM MgCl<sub>2</sub> added to stabilize the structure (entry 7).<sup>9</sup> Here, only a slight destabilization by the unconventional nucleosides is observed. However, this is also evident for the oligonucleotide containing an abasic site at the junction (**ON6**), indicating that canonical base pairing is not an important structural factor in this motif. As indicated by Seemann and co-workers, it is probably not possible to form all canonical base pairs at the branch point in a DNA three-way junction.<sup>28</sup> Hence, the DNA three-way junction is known to display a flexible structure, a trait which may be imparted by incorporating a dinucleotide bulge adjacent to the structural branch point.<sup>29,30</sup> Therefore, we employed the same three-way motif with a CC bulge adjacent to the junction to render a less flexible motif (entry 8).<sup>11,13</sup> The results suggest, however, that the double-headed modifications do not fit in the motif, as

the destabilizations are larger and the differences between the abasic site and the double-headed nucleosides are again of minor importance.

The results obtained for the RNA based motifs are also given in Table 2. With an unbulged RNA complement (entry 9), **ON2** forms a duplex, which is more destabilized by approx. -3 °C compared to the duplex formed by **ON5** incorporating the GNA thymidine analog. Compared to the native duplex, however, **ON2** is less destabilized in an RNA environment than in the DNA environment (-8 °C compared to -10 °C). This is not surprising as GNA has been shown to cross-pair with RNA but not with DNA.<sup>17</sup> The effect, however, appears to be less pronounced for the other three stereoisomers in **ON1**, **ON3** and **ON4** and the abasic site in **ON6**. Again, it is particularly interesting that **ON2** is observed to form more stable duplexes than **ON3** with a difference of 3 °C. This is a clear indication that the orientation of the extra methyl linker moiety at C3' is important for the accommodation of the extra thymine base in a duplex structure.

While the bulged RNA motifs display destabilized structures without significant stereochemical influence, similar to the DNA congener (entries 10–11), the stability of the RNA three-way junction is observed to be very dependent on the stereochemistry of the double-headed nucleosides (entry 12). Indeed, **ON4** stabilizes this RNA motif by +2 °C without MgCl<sub>2</sub> whereas the other oligonucleotides destabilize the motif by -2 °C to -3 °C. This property is seen to be true in both medium and high concentrations of NaCl. Although the observed stabilization for **ON4** seems to level off with increasing concentration of MgCl<sub>2</sub>, the differences from the stereochemical relationship are almost constant. Although the stabilization is modest, the fairly large difference (which is dependent on stereochemistry) indicates that this motif is not unduly flexible and that it is possible to target and stabilize the secondary structure with a designed molecule. Indeed, **ON4**, which shows the best fit into the RNA three-way junction,

incorporates a nucleoside that is the mirror image of the nucleoside incorporated into **ON2**, found to be the better oligonucleotide in simple duplex formation.

## Discussion

The synthesis of the four stereoisomeric double-headed nucleosides was fairly simple. The two *threo*-configured phosphoramidites were obtained in only four steps from cheap commercially available starting materials, and the *erythro*-configured analogs demanded only two additional steps. On the other hand, the preparation of the latter was based on the so-called anhydro approach, which is only possible with the pyrimidine nucleobases. Therefore, the procedure would not be immediately useful for the preparation of *erythro*-configured purine analogs. In contrast to the relatively easy preparation of the phosphoramidites, their oligomerisation was a challenging task. The kinetic studies proved that pyrHCl is the preferred activator for these amidites and that the incorporation can be performed with reasonable efficiency. Nevertheless, steric problems in the coupling step and the ring-closure during the detritylation and subsequent coupling step hamper the incorporation of the *threo*-configured amidites so much that more than single incorporations in the ODNs were impossible. On the other hand, the *erythro*-configured amidites were more efficiently incorporated, and a direct study of the cooperativity between the double-headed acyclic nucleosides and their GNA counterparts can thus be performed in the near future.

Compared to other double-headed nucleosides studied by us and others,<sup>8–11</sup> the four stereoisomeric acyclic nucleosides of this study display the most pronounced destabilization of duplexes. In other words, the combination of conformational flexibility, a backbone that is shortened by one carbon atom, and an additional base is not optimal for duplex formation. It is not surprising, however, that an intact 2'-deoxyribose skeleton (as in **1–3**) is preferred, as single incorporations of the GNA-monomers into duplexes are also known to induce significant destabilizations.<sup>14</sup> For that reason, the effect of additional bases in fully modified GNA-sequences might give completely different results. The different stereochemistries give, however, some differences in the destabilization of duplexes, and the most "GNA-like" analog (as in **ON2**, Table 2), with the 2'(*S*)-configuration of GNA and the additional thymine pointing away from the duplex (Fig. 4a), shows almost the same thermal stability as the GNA-sequence (**ON5**). The study of a 5'-positioned (thymine-1-yl)methyl group using the double-headed nucleoside **2** has recently shown an intriguing interstrand base–base interaction in a DNA-zipper motif.<sup>11</sup> A similar effect of the (thymine-1-yl)methyl group of the *D-erythro*-configured compound **14** in a corresponding GNA-zipper motif might be envisioned.

The study of three-way junctions has demonstrated that it is impossible to obtain large increases in thermal stability by simple and flexible acyclic double-headed nucleosides in the model system studied. On the other hand, the four different stereochemical configurations have demonstrated some influence, as one of them actually gives a slight stabilization of the DNA–RNA three-way junction. However, the three-way junction is not really very stable, and the stabilization obtained with the double-headed nucleoside **1** in the presence of Mg<sup>2+</sup> was significantly more powerful. The TWJ stabilization obtained with one of the four stereoisomers

indicates an important effect on TWJ structure of one or rather both of the nucleobases.

## Conclusion

A set of four diastereomeric 1,4-bis(thymine-1-yl)butane-2,3-diols has been prepared and incorporated into oligonucleotides. In general, the nucleosides destabilize both DNA and RNA duplexes. However, not unexpectedly the nucleosides bearing an 2'(*S*)-configuration are marginally less destabilising. This is also true for bulged motifs. For the three-way junctions formed with DNA no proper indication of base pairing at the junction was observed. However, in the case of three-way junctions formed with RNA it is found that the stereochemistry of the nucleosides is important, as one of the nucleosides demonstrates a stabilization effect, while the others display a varying degree of destabilization in a consistent manner when varying the Mg<sup>2+</sup> and the Na<sup>+</sup> concentrations. In essence, these results demonstrate the possibility of targeting and stabilizing nucleic acid secondary structures with suitably designed nucleosides and oligonucleotides.

## Experimental

Reactions were carried out under an atmosphere of nitrogen when anhydrous solvents were used. Column chromatography was carried out using glass columns with silica gel 60 (0.040–0.063 mm). NMR spectra were recorded on Varian Gemini 2000 spectrometers. NMR spectra were recorded at 300 or 200 MHz for <sup>1</sup>H NMR, 75 or 50 MHz for <sup>13</sup>C NMR and 121.5 or 81 MHz for <sup>31</sup>P NMR. The  $\delta$  values are in ppm relative to tetramethylsilane as internal standard (for <sup>1</sup>H and <sup>13</sup>C NMR) and relative to 85% H<sub>3</sub>PO<sub>3</sub> as external standard (for <sup>31</sup>P NMR). Assignments of NMR spectra are based on 2D experiments and DEPT. HR MALDI and ESI mass spectra were recorded in positive-ion mode except for the oligonucleotides, which were recorded in negative-ion mode. Optical rotation was recorded on a Perkin Elmer Model 141 polarimeter.

### Preparation of (2*R*,3*R*)-1,4-bis(3-*N*-benzoylthymine-1-yl)-butan-2,3-diol (**6a**)

3-*N*-Benzoylthymine (1.6 g, 6.9 mmol), 2,3-*O*-isopropylidene-*D*-threitol **5a** (0.52 g, 3.2 mmol) and triphenylphosphine (2.6 g, 9.9 mmol) were dissolved in anhydrous THF (50 mL) and the solution was stirred at room temperature. When all the compounds had dissolved, the solution was cooled to 0 °C and DEAD (1.5 mL, 10 mmol) was added over 15 minutes. The mixture was stirred for 16 h at room temperature and then concentrated under reduced pressure at 30 °C. The residue was purified by silica gel column chromatography (CHCl<sub>3</sub>–EtOH 99 : 1 v/v) to give a crude intermediate containing triphenylphosphine oxide. This intermediate was dissolved in a mixture of trifluoroacetic acid and water (3 : 1, 20 mL) and the solution was stirred for 4.5 h. The reaction was quenched by the addition of a saturated aqueous solution of NaHCO<sub>3</sub> (170 mL) and the mixture was extracted with CHCl<sub>3</sub> (4 × 20 mL). The combined organic phases were dried (MgSO<sub>4</sub>) and the solvent was removed under reduced pressure. The residue was purified by silica gel column chromatography (EtOAc–petrol ether 1 : 1 v/v, to remove triphenylphosphine

oxide, and then  $\text{CHCl}_3$ –EtOH 19 : 1 v/v). The residue was finally precipitated from  $\text{CHCl}_3$  by the slow addition of hexane to give the product **6a** as a white powder (0.88 g, 50%).  $R_f$  0.35 ( $\text{CHCl}_3$ –EtOH 9 : 1);  $\delta_H$  (300 MHz, DMSO- $d_6$ , Me $_4$ Si) 7.94–7.91 (4H, m, Ar H), 7.79–7.73 (2H, m, Ar H), 7.69 (2H, d,  $J$  = 0.9 Hz, H-6), 7.60–7.55 (4H, m, Ar H), 5.31 (2H, d,  $J$  = 5.7 Hz, OH), 3.93–3.65 (6H, m, H-1', H-1'', H-2'), 1.83 (6H, d,  $J$  = 0.9 Hz, 2  $\times$  CH $_3$ ),  $\delta_C$  (75 MHz, DMSO- $d_6$ , Me $_4$ Si) 169.70 (C-4), 162.89 (PhC=O), 149.52 (C-2), 143.59 (C-6), 135.26, 131.17, 130.13, 129.34 (Ar C), 107.50 (C-5), 68.58 (CH), 51.04 (CH $_2$ ), 11.76 (CH $_3$ ); HR MALDI MS  $m/z$  569.1667 ([M + Na] $^+$ , C $_{28}$ H $_{26}$ N $_4$ O $_8$ Na calcd 569.1643).

#### Preparation of (2*S*,3*S*)-1,4-bis(3-*N*-benzoylthymine-1-yl)-butan-2,3-diol (**6b**)

Same procedure as above. 2,3-*O*-Isopropylidene-L-threitol (0.888 g) was used to give the product **6b** as a white powder (1.07 g, 36%). NMR data are identical to data for the enantiomer **6a**; HR MALDI MS  $m/z$  569.1641 [M + Na] $^+$ .

#### Preparation of (2*R*,3*R*)-1,4-bis(3-*N*-benzoylthymine-1-yl)-3-(4,4-dimethoxytrityloxy)butan-2-ol (**7a**)

The diol **6a** (0.77 g, 1.4 mmol) was co-evaporated with anhydrous pyridine (3  $\times$  6 mL) and redissolved in anhydrous pyridine (9 mL). DMTCl (1.2 g, 3.5 mmol) was added and the mixture was stirred for 16 h. Another portion of DMTCl (0.59 g, 1.7 mmol) was added and the mixture was stirred for another 24 h. The reaction mixture was diluted with EtOAc (40 mL) and washed with water (150 mL). The water phase was extracted with EtOAc (40 mL) and the combined organic fractions were dried (Na $_2$ SO $_4$ ) and concentrated under reduced pressure. The residue was purified by silica gel column chromatography ( $\text{CHCl}_3$ –petrol ether 1 : 1 v/v containing 0.2% Et $_3$ N) to give the product **7a** as a powder binding 2.5 equivalents of Et $_3$ N (0.89 g, 74%).  $R_f$  0.60 ( $\text{CHCl}_3$ –EtOH 9 : 1);  $\delta_H$  (300 MHz, DMSO- $d_6$ , Me $_4$ Si) 7.92–7.81 (4H, m, Ar H), 7.66–7.59 (2H, m Ar H), 7.51–7.40 (10H, m, Ar H), 7.33–7.23 (4H, m Ar H), 7.15 (1H, d,  $J$  = 1.2 Hz, H-6), 6.88–6.84 (4H, m, Ar H), 6.32 (1H, s, H-6), 4.23 (1H, d,  $J$  = 13.5 Hz), 3.98 (1H, m), 3.90–3.85 (2H, m), 3.78 (6H, s), 3.68 (1H, dd,  $J$  = 3.9, 13.5 Hz), 3.58 (1H, m), 3.29 (1H, dd,  $J$  = 3.0, 13.8 Hz), 1.86 (3H, s, CH $_3$ ), 1.81 (3H, s, CH $_3$ ).  $\delta_C$  (75 MHz, DMSO- $d_6$ , Me $_4$ Si) 169.20, 168.56 (C-4), 157.85 (Ar C), 150.70, 146.57 (C-2), 143.15, 141.92 (C-6), 136.36, 136.14, 129.60, 127.43, 127.36, 126.19, 112.81 (Ar C), 111.67, 109.93 (C-5), 87.48 (C(Ar) $_3$ ), 73.17, 69.75 (CH), 55.42 (OCH $_3$ ), 51.04, 47.00 (CH $_2$ ), 12.39, 12.36 (CH $_3$ ).

#### Preparation of (2*S*,3*S*)-1,4-bis(3-*N*-benzoylthymine-1-yl)-3-(4,4-dimethoxytrityloxy)butan-2-ol (**7b**)

Same procedure as above. Diol **6b** (0.13 g) was used to give the product **7b** as a powder binding 2.5 equivalents of Et $_3$ N (0.16 g, 77%). NMR data are identical to data for the enantiomer **7a**.

#### Preparation of (2*R*,3*R*)-1,4-bis(3-*N*-benzoylthymine-1-yl)-3-(4,4-dimethoxytrityloxy)but-2-oxy- $\beta$ -cyanoethoxy-*N,N*-diisopropylaminophosphite (**8a**)

Compound **7a** (1.75 g, 2.06 mmol) was dissolved in anhydrous  $\text{CH}_2\text{Cl}_2$  (10 mL) and to the solution was added diiso-

propylethylamine (2.0 mL, 12 mmol) followed by chloro-(2-cyanoethoxy)(diisopropylamino)phosphane (1.0 g, 4.2 mmol). The mixture was stirred at room temperature for 1 h, diluted with EtOAc (50 mL) and washed with brine (4  $\times$  25 mL). The organic phase was dried (Na $_2$ SO $_4$ ) and concentrated under reduced pressure. The residue was purified by silica gel column chromatography (EtOAc–Et $_3$ N 99 : 1 v/v). The residual compound was dissolved in  $\text{CH}_2\text{Cl}_2$  (2 mL) and precipitated into hexane (20 mL) overnight at  $-20$  °C to give the product **8a** as a white powder (1.43 g, 64%).  $R_f$  0.66 (EtOAc–Et $_3$ N 99 : 1);  $\delta_P$  (121 MHz, CDCl $_3$ ) 152.13, 149.73; HR MALDI MS  $m/z$  1071.4007 ([M + Na] $^+$ , C $_{58}$ H $_{62}$ N $_6$ O $_{11}$ PNa calcd 1071.4028).

#### Preparation of (2*S*,3*S*)-1,4-bis(3-*N*-benzoylthymine-1-yl)-3-(4,4-dimethoxytrityloxy)but-2-oxy- $\beta$ -cyanoethoxy-*N,N*-diisopropylaminophosphite (**8b**)

Same procedure as above. Compound **7b** (125 mg) was used to give the product **8b** as a white powder (61 mg, 39%).  $\delta_P$  (121 MHz, CDCl $_3$ ) 152.15, 149.74; HR MALDI MS  $m/z$  1071.4072 [M + Na] $^+$ .

#### Preparation of (2*R*,3*R*)-1,4-bis(thymine-1-yl)-3-(4,4-dimethoxytrityloxy)butan-2-ol (**9a**)

3-*N*-Benzoylthymine (12.80 g, 55.6 mmol), 2,3-*O*-isopropylidene-D-threitol **5a** (4.03 g, 24.9 mmol) and triphenylphosphine (23.1 g, 88.2 mmol) were dissolved in anhydrous THF (400 mL). The solution was stirred at rt for 30 min, cooled to 0 °C and a 40% w/w solution of DEAD in toluene (40 mL, 87 mmol) added over 15 min. The mixture was stirred at rt for 16 h and concentrated under reduced pressure. The residue was dissolved in a mixture of trifluoroacetic acid and water (3 : 1 v/v, 100 mL) and stirred for 5 h. The mixture was diluted with water (300 mL) and neutralized by slow addition of Na $_2$ CO $_3$  (53 g). The mixture was extracted with  $\text{CHCl}_3$  (4  $\times$  100 mL), and the combined extracts were dried (MgSO $_4$ ) and concentrated under reduced pressure. The residue was purified by column chromatography ( $\text{CHCl}_3$ –EtOH 19 : 1 v/v). The residue was dried under vacuum for 16 h and then dissolved in anhydrous pyridine (100 mL). DMTCl (4.9 g, 15 mmol) was added and the mixture was stirred for 24 h; another portion of DMTCl (3.5 g, 10 mmol) was then added and the mixture stirred for another 24 h. The mixture was concentrated under reduced pressure, and the residue was suspended in a mixture of 1,4-dioxane (100 mL) and a 2 M aqueous solution of NaOH (100 mL). The mixture was stirred for 2 d and neutralized by the addition of neat AcOH (12 mL). Brine (100 mL) was added and the mixture was extracted with EtOAc (3  $\times$  100 mL). The combined extracts were dried (Na $_2$ SO $_4$ ) and concentrated under reduced pressure. The residue was purified by column chromatography (EtOAc–petrol ether 1 : 1 v/v containing 0.2 vol% Et $_3$ N, then  $\text{CH}_2\text{Cl}_2$ –MeOH 19 : 1 v/v containing 0.2 vol% Et $_3$ N) to give the product **9a** as a white powder (1.68 g, 11% over the four steps).  $R_f$  0.36 ( $\text{CHCl}_3$ –EtOH 9 : 1);  $\delta_H$  (300 MHz, DMSO- $d_6$ , Me $_4$ Si) 11.15 (1H, s, NH) 11.12 (1H, s, NH), 7.38–7.08 (10H, m, Ar H and H-6), 6.76–6.69 (4H, Ar H), 5.48 (1H, d  $J$  = 4.8 Hz, OH), 4.01–3.81 (3H, m), 3.72 (6H, s, 2  $\times$  OCH $_3$ ), 3.60–3.50 (1H, m), 3.21–3.17 (1H, m), 1.63 (3H, s, CH $_3$ ), 1.48 (3H, s, CH $_3$ );  $\delta_C$  (75 MHz, DMSO- $d_6$ , Me $_4$ Si) 164.27, 164.13 (C-4), 157.85



(Ar C), 150.70, 146.57 (C-2), 143.15, 141.92 (C-6), 136.36, 136.14, 129.60, 127.43, 127.36, 126.19, 112.81 (Ar C), 108.09, 106.96 (C-5), 86.57 (C(Ar)<sub>3</sub>), 72.41, 67.60 (CH), 54.81 (OCH<sub>3</sub>), 50.23, 47.59 (CH<sub>2</sub>), 11.49, 11.44 (CH<sub>3</sub>); HR ESI MS *m/z* 663.2768 ([M + Na]<sup>+</sup>, C<sub>35</sub>H<sub>36</sub>N<sub>4</sub>O<sub>8</sub>Na calcd 663.2453). [α]<sub>D</sub><sup>25</sup> = +86 (*c* = 1.00 g mL<sup>-1</sup>, DMSO-*d*<sub>6</sub>).

#### Preparation of (2*S*,3*S*)-1,4-bis(thymin-1-yl)-3-(4,4-dimethoxytrityloxy)butan-2-ol (9b)

Same procedure as above. 2,3-*O*-Isopropylidene-L-threitol **5b** (3.06 g) was used to give the product **9b** as a white powder (2.14 g, 18%). NMR data are identical to data for the enantiomer **9a**; HR ESI MS *m/z* 663.2472 [M + Na]<sup>+</sup>. [α]<sub>D</sub><sup>25</sup> = -83 (*c* = 1.00 g mL<sup>-1</sup>, DMSO-*d*<sub>6</sub>).

#### Preparation of (2*R*,3*R*)-1,4-bis(3-*N*-benzoylthymin-1-yl)-3-(4,4-dimethoxytrityloxy)but-2-yl methansulfonate (10a)

Compound **9a** (1.38 g, 2.15 mmol) was dissolved in anhydrous pyridine (70 mL), and the reaction mixture was stirred at 0 °C. MsCl (0.50 mL, 6.4 mmol) was added slowly, and the reaction mixture was stirred for 3 h, another portion of MsCl (0.50 mL, 6.4 mmol) added, stirred for 4 h, then added another portion of MsCl (0.50 mL, 6.4 mmol) and stirred for 12 h. The mixture was quenched in water (100 mL) and extracted with CH<sub>2</sub>Cl<sub>2</sub> (4 × 40 mL). The combined extracts were washed with brine (100 mL), dried (Na<sub>2</sub>SO<sub>4</sub>) and concentrated under reduced pressure. The residue was purified by column chromatography (CH<sub>2</sub>Cl<sub>2</sub>-MeOH 98:2 v/v containing 0.2 vol% Et<sub>3</sub>N) to give a brown oil, which was dissolved in CH<sub>2</sub>Cl<sub>2</sub> (3 mL) and precipitated into hexane (30 mL) to give the product **10a** as a white powder (0.640 g, 41%). *R*<sub>f</sub> 0.33 (CHCl<sub>3</sub>-EtOH 9 : 1); δ<sub>H</sub> (300 MHz, DMSO-*d*<sub>6</sub>, Me<sub>4</sub>Si) 11.35 (1H, s, N-H), 11.06 (1H, s, N-H), 7.43-7.40 (2H, m, Ar H), 7.31-7.20 (8H, m, Ar H), 7.09 (1H, s, H-6), 6.86-6.80 (4H, m, Ar H), 4.61-4.57 (1H, m), 4.52 (1H, dd, *J* = 2.1, 14.7 Hz), 4.10-3.91 (3H, m), 3.74 (6H, s, 2 × OCH<sub>3</sub>), 3.68-3.63 (1H, m), 2.87 (3H, s, CH<sub>3</sub>SO<sub>3</sub>), 1.73 (3H, s, CH<sub>3</sub>), 1.56 (3H, s, CH<sub>3</sub>); δ<sub>C</sub> (75 MHz, DMSO-*d*<sub>6</sub>, Me<sub>4</sub>Si) 164.19, 164.09 (C-4), 158.40, 158.38 (Ar), 150.94, 150.60 (C-2), 145.36 (Ar), 141.72, 141.61 (C-6), 135.10, 135.02, 130.50, 130.38, 127.93, 127.80, 126.93, 113.21, 113.09 (Ar), 108.54, 108.21 (C-5), 87.73 (C(Ar)<sub>3</sub>), 77.72, 70.01 (CH), 55.04, 54.92 (OCH<sub>3</sub>), 47.84, 45.71 (CH<sub>2</sub>), 38.08 (CH<sub>3</sub>SO<sub>3</sub>), 11.90, 11.71 (CH<sub>3</sub>); HR ESI MS *m/z* 741.2226 ([M + Na]<sup>+</sup>, C<sub>36</sub>H<sub>38</sub>N<sub>4</sub>O<sub>10</sub>SNa calcd 741.2201).

#### Preparation of (2*S*,3*S*)-1,4-bis(3-*N*-benzoylthymin-1-yl)-3-(4,4-dimethoxytrityloxy)but-2-yl methansulfonate (10b)

Same procedure as above. Compound **9b** (1.84 g) was used to give the product **10b** as a white powder (1.04 g, 50%). NMR data are identical to data for the enantiomer **10a**. HR ESI MS *m/z* 741.2231 [M + Na]<sup>+</sup>.

#### Preparation of (2*S*,3*R*)-1,4-bis(thymin-1-yl)-3-(4,4-dimethoxytrityloxy)butan-2-ol (11a)

Compound **10a** (0.421 g, 0.586 mmol) was dissolved in a mixture of EtOH (9 mL) and a 1 M aqueous solution of NaOH (9 mL) and the mixture stirred at reflux for 4 h. After cooling to room

temperature, the mixture was neutralized with AcOH (approx. 0.5 mL) and diluted with water (20 mL). The mixture was extracted with CH<sub>2</sub>Cl<sub>2</sub> (4 × 20 mL), and the combined extracts were dried (Na<sub>2</sub>SO<sub>4</sub>) and concentrated under reduced pressure. The residue was purified by column chromatography (CH<sub>2</sub>Cl<sub>2</sub>-MeOH 98 : 2 v/v containing 0.2 vol% Et<sub>3</sub>N) to give the product **11a** as a white powder (0.314 g, 84%). *R*<sub>f</sub> 0.55 (CHCl<sub>3</sub>-EtOH 9 : 1); δ<sub>H</sub> (200 MHz, DMSO-*d*<sub>6</sub>, Me<sub>4</sub>Si) 11.15 (1H, s, N-H), 11.12 (1H, s, N-H), 7.38-7.08 (10H, m, Ar H and H-6), 6.76-6.69 (4H, Ar H), 5.48 (1H, d, *J* = 6.6 Hz, OH), 4.01-3.81 (3H, m), 3.72 (6H, s, 2 × OCH<sub>3</sub>), 3.60-3.50 (1H, m), 3.21-3.17 (1H, m), 1.63 (3H, s, CH<sub>3</sub>), 1.48 (3H, s, CH<sub>3</sub>); δ<sub>C</sub> (50 MHz, DMSO-*d*<sub>6</sub>, Me<sub>4</sub>Si) 164.27, 164.13 (C-4), 157.85 (Ar C), 150.70, 146.57 (C-2), 143.15, 141.92 (C-6), 136.36, 136.14, 129.60, 127.43, 127.36, 126.19, 112.81 (Ar C), 108.09, 106.96 (C-5), 86.57 (C(Ar)<sub>3</sub>), 72.41, 67.60 (CH), 54.81 (OCH<sub>3</sub>), 50.23, 47.59 (CH<sub>2</sub>), 11.49, 11.44 (CH<sub>3</sub>); HR ESI MS *m/z* 663.2473 ([M + Na]<sup>+</sup>, C<sub>35</sub>H<sub>36</sub>N<sub>4</sub>O<sub>8</sub>Na calcd 663.2453). [α]<sub>D</sub><sup>25</sup> = +107 (*c* = 1.00 g mL<sup>-1</sup>, DMSO-*d*<sub>6</sub>).

#### Preparation of (2*R*,3*S*)-1,4-bis(thymin-1-yl)-3-(4,4-dimethoxytrityloxy)butan-2-ol (11b)

Same procedure as above. Compound **10b** (0.91 g) was used to give the product **11b** as a white powder (0.71 g, 88%). NMR data are identical to data for the enantiomer **11a**. HR ESI MS *m/z* 663.2442 [M + Na]<sup>+</sup>. [α]<sub>D</sub><sup>25</sup> = -104 (*c* = 1.00 g mL<sup>-1</sup>, DMSO-*d*<sub>6</sub>).

#### Preparation of (2*S*,3*R*)-1,4-bis(3-*N*-benzoylthymin-1-yl)-3-(4,4-dimethoxytrityloxy)but-2-oxy-β-cyanoethoxy-*N,N*-diisopropylaminophosphite (12a)

Compound **11a** (0.311 g, 0.486 mmol) was dissolved in anhydrous CH<sub>2</sub>Cl<sub>2</sub> (10 mL) and diisopropylethylamine (0.60 mL), and chloro-2-cyanoethoxydiisopropylaminophosphane (0.30 g, 1.3 mmol) was added. The mixture was stirred at room temperature for 1 h, transferred directly onto a column and purified by chromatography (EtOAc containing 0.2 vol% Et<sub>3</sub>N) to give the product **12a** as a white powder (0.281 g, 69%). δ<sub>P</sub> (121 MHz, CDCl<sub>3</sub>) 151.29, 151.17; HR ESI MS *m/z* 863.3486 ([M + Na]<sup>+</sup>, C<sub>44</sub>H<sub>53</sub>N<sub>6</sub>O<sub>9</sub>PNa calcd 863.3504).

#### Preparation of (2*R*,3*S*)-1,4-bis(3-*N*-benzoylthymin-1-yl)-3-(4,4-dimethoxytrityloxy)but-2-oxy-β-cyanoethoxy-*N,N*-diisopropylaminophosphite (12b)

Same procedure as above. Compound **11b** (0.59 g) was used to give the product **12b** as a white powder (0.50 g, 64%). NMR data are identical to data for the enantiomer **12a**. HR ESI MS *m/z* 863.3494 [M + Na]<sup>+</sup>.

#### Synthesis of (2*R*,3*R*)-1,4-bis(thymin-1-yl)butane-2,3-diol (13)

A small amount of compound **9a** was dissolved in a little CH<sub>2</sub>Cl<sub>2</sub> and suspended with silica. A few drops of dichloroacetic acid were added and the mixture was stirred for 10 min and concentrated under reduced pressure. The powder was purified by chromatography on a Pasteur pipette column (CHCl<sub>3</sub>-EtOH 4 : 1 v/v) to give the crude product. This was dissolved in a small amount of DMSO in an open vial and placed in a closed beaker

with water to give crystals after a few days.  $\delta_{\text{H}}$  (300 MHz, DMSO- $d_6$ , Me<sub>4</sub>Si) 11.21 (2H, s, N-H), 7.41 (2H, s, H-6), 5.10 (2H, d,  $J = 6$  Hz, OH), 3.80 (2H, dd,  $J = 2$  Hz, 13 Hz, H-1'), 3.66 (2H, m, H-2'), 3.55 (2H, dd,  $J = 9$  Hz, 13 Hz, H-1''), 1.75 (6H, s, CH<sub>3</sub>).

#### Synthesis of *meso*-1,4-bis(thymin-1-yl)butan-2,3-diol (**14**)

Similar reaction procedure as above, but using **11a**. The crude product was dissolved in a little DMSO and evaporated under reduced pressure at 100 °C until crystals appeared. Then, the crystal growth was allowed to proceed while slowly cooling down to room temperature over 5 h.  $\delta_{\text{H}}$  (300 MHz, DMSO- $d_6$ , Me<sub>4</sub>Si) 11.19 (2H, s, N-H), 7.41 (2H, s, H-6), 5.25 (2H, br s, OH), 4.09 (2H, d,  $J = 13$  Hz, H-1'), 3.55 (2H, m, H-2'), 3.35 (2H, dd,  $J = 8$  Hz, 13 Hz, H-1''), 1.74 (6H, s, CH<sub>3</sub>).

#### Synthesis of a model dinucleotide and <sup>31</sup>P-NMR study of the detritylation step

A solution of **8a** (0.66 g, 0.63 mmol) and 3'-*O*-(*tert*-butyldimethylsilyl)thymidine (0.27 g, 0.75 mmol) in anhydrous MeCN (2.0 mL) was stirred at room temperature and a 0.5 M solution of pyrHCl in MeCN (2.0 mL, 1 mmol) was added. The mixture was stirred for 20 h, and a 5.5 M solution of *t*-BuOOH in decane (0.2 mL, 1 mmol) was added. The mixture was stirred for 1 h and directly purified by column chromatography (CH<sub>2</sub>Cl<sub>2</sub>–MeOH 99 : 1 v/v containing 0.5 vol% pyridine). The residue was co-evaporated with a xylene mixture and dried under reduced pressure to give the dinucleotide product as a white compound (0.43 g, 57%).  $R_f$  0.55 (CH<sub>2</sub>Cl<sub>2</sub>–MeOH 19 : 1); <sup>31</sup>P-NMR (81 MHz, CDCl<sub>3</sub>)  $\delta$  0.03, –0.36. The kinetics were acquired as follows: the dinucleotide (0.191 g, 0.159 mmol) was dissolved in CD<sub>2</sub>Cl<sub>2</sub> (0.50 mL) in an NMR tube. A solution of trichloroacetic acid (26 mg, 0.16 mmol) in CD<sub>2</sub>Cl<sub>2</sub> (234 mg) was added to initiate the reaction. Spectra recorded in 256 s were acquired in the spectral window from  $\delta = 100$  to –100 ppm.

#### Oligonucleotide synthesis

The oligonucleotides were synthesized on an automated DNA synthesizer Expedite 8909 on a 0.2  $\mu$ mol scale using CPG support and employing a standard phosphoramidite protocol except for the couplings involving the unconventional nucleosides. These were coupled manually by treating the CPG support with a 0.05 M mixture of the phosphoramidite in acetonitrile (100  $\mu$ L) and a 0.5 M solution of activator (1*H*-tetrazole or pyridinium chloride) in acetonitrile (100  $\mu$ L) for 10 minutes. Resuming the automatic cycle, the support was washed and capped according to the standard protocol and then again manually treated with a mixture of acetonitrile (300  $\mu$ L) and a 5.5 M solution of *t*-BuOOH in decane (100  $\mu$ L) for 5 minutes. The next elongation was conducted according to the standard protocol except for a prolonged coupling time of 15 minutes. The oligonucleotides were removed from the support and deprotected by treatment with a 32% w/w aqueous NH<sub>3</sub> solution (1 mL) at 55 °C for 16 h. Subsequent purification was performed using reversed HPLC (column XTerra C18, 10 mm, 7.8  $\times$  300 mm, with a gradient of buffers A and B (A, 90% 0.1 M NH<sub>4</sub>HCO<sub>3</sub> + 10% CH<sub>3</sub>CN; B, 25% 0.1 M NH<sub>4</sub>HCO<sub>3</sub> + 75% CH<sub>3</sub>CN), 1 mL min<sup>–1</sup>), and detritylation

was performed using aqueous acetic acid. Precipitation with EtOH afforded the oligonucleotides.

#### Thermal denaturation experiments

The thermal denaturation studies were conducted in a medium salt buffer containing Na<sub>2</sub>HPO<sub>4</sub> (10 mM), NaCl (100 mM) and EDTA (0.1 mM), pH 7.0 with 1  $\mu$ M concentrations of the two strands. The concentrations were determined assuming the unconventional double-headed nucleosides to have an extinction coefficient twice the normal thymidines. The hyperchromicity was measured as a function of time while increasing the temperature linearly between 10 and 80 °C at a time rate of 1 °C min<sup>–1</sup>. The melting temperature was then determined as the maximum of the first derivative of the hyperchromicity. Probes with both up and down curves were in general found to be identical.

#### X-Ray crystallography

Single-crystal X-ray diffraction data for **13**·DMSO·2H<sub>2</sub>O were collected at 180(2) K using a Bruker-Nonius X8APEX-II CCD diffractometer, with MoK $\alpha$  radiation ( $\lambda = 0.7107$  Å). Incorporation of DMSO into the crystal allowed the absolute structure to be confirmed on the basis of the diffraction data. Crystals of **14**·2DMSO were small and weakly diffracting, and diffraction data were collected at 150(2) K at Beamline I911-3 of the MAX-II storage ring at MAX-Lab, Lund, Sweden ( $\lambda = 0.7500$  Å). On account of experimental constraints, data were collected using only a single 360°  $\phi$  scan, resulting in *ca.* 88% completeness to a resolution of 1 Å. Data were corrected for beam decay during integration on the basis of ring-current values using the TWINOLVE package.<sup>31</sup> Both structures were solved and refined using SHELXTL.<sup>32</sup> H atoms bonded to C atoms were placed geometrically and refined using a riding model. For **13**, H atoms bonded to O atoms were located in difference Fourier maps and refined with restrained O–H distances and isotropic displacement parameters constrained to be 1.2 or 1.5 times the equivalent isotropic displacement parameter of the O atom to which they are bonded. For **14**, the H atom of the unique hydroxyl group was placed so as to form a linear O–H...O hydrogen bond to the incorporated DMSO molecule, and refined as riding with an isotropic displacement parameter constrained to be 1.5 times the equivalent isotropic displacement parameter of the parent O atom. The data and resulting structure of **14**·2DMSO are of comparatively low quality, but are sufficient to establish the *meso*-configuration.

**Crystal data for 13·DMSO·2H<sub>2</sub>O.** C<sub>16</sub>H<sub>28</sub>N<sub>4</sub>O<sub>9</sub>S,  $M_w = 452.48$  g mol<sup>–1</sup>, crystal dimensions 0.20  $\times$  0.14  $\times$  0.12 mm, monoclinic, space group *P*2<sub>1</sub>,  $a = 5.2709(12)$ ,  $b = 16.736(4)$ ,  $c = 12.148(3)$  Å,  $\beta = 97.432(4)^\circ$ ,  $V = 1062.6(4)$  Å<sup>3</sup>,  $Z = 2$ ,  $\rho_{\text{calcd}} = 1.414$  g cm<sup>–3</sup>,  $\mu(\text{MoK}\alpha) = 0.208$  mm<sup>–1</sup>,  $3.60 < 2\theta < 26.13^\circ$ ; of 9515 measured reflections, 4139 were independent ( $R_{\text{int}} = 0.029$ ) and 3634 observed with  $I > 2\sigma(I)$ ;  $R1 = 0.049$ ,  $wR2 = 0.138$ , GOF = 1.07 for 291 parameters and 10 restraints, Flack parameter = –0.06(10),  $\Delta\rho_{\text{max/min}} = 0.99/–0.39$ . CCDC reference number 643524. For crystallographic data in CIF or other electronic format see DOI: 10.1039/b713888a

**Crystal data for 14-2DMSO.**  $C_{18}H_{30}N_4O_8S_2$ ,  $M_w = 494.58$  g mol<sup>-1</sup>, crystal dimensions  $0.10 \times 0.02 \times 0.02$  mm, triclinic, space group  $P\bar{1}$ ,  $a = 5.224(2)$ ,  $b = 9.313(4)$ ,  $c = 12.558(6)$  Å,  $\alpha = 101.76(3)$ ,  $\beta = 91.68(3)$ ,  $\gamma = 105.00(3)^\circ$ ,  $V = 575.6(4)$  Å<sup>3</sup>,  $Z = 1$ ,  $\rho_{\text{calcd}} = 1.427$  g cm<sup>-3</sup>,  $\mu(\lambda = 0.7500 \text{ Å}) = 0.283$  mm<sup>-1</sup>,  $4.32 < 2\theta < 22.03^\circ$ ; of 1231 measured reflections, 1047 were independent ( $R_{\text{int}} = 0.025$ ) and 918 observed with  $I > 2\sigma(I)$ ;  $R1 = 0.117$ ,  $wR2 = 0.316$ ,  $GOF = 3.02$  for 145 parameters,  $\Delta\rho_{\text{max/min}} = 0.90/-0.54$ . CCDC reference number 643525. For crystallographic data in CIF or other electronic format see DOI: 10.1039/b713888a

## Molecular modelling

MD-simulation was performed with the Amber99 force field with parameters as supplied with Amber7.<sup>33</sup> The coordinates for the B-DNA were obtained from 1n1o.pdb, where one of the TNA monomers was replaced with the ordinary T monomer and the other replaced with the double-headed glycol nucleosides. The partial charges were derived using *resp* and the rhf/6-31g\* wave function obtained from a GAMESS<sup>34</sup> run using the nucleoside coordinates from a MMFF94 force field minimization of the 2',3'-*O*-methyl analogs. The duplexes were neutralised with 10 Na<sup>+</sup> and placed in a 7.0 Å truncated octahedron with TIP3P waters. Using Sander with PBC and PME, the systems were then allowed to relax with 1000 minimisation steps using a 8 Å cutoff for the non-bonded potential terms and a 500 kcal mol<sup>-1</sup> Å<sup>-2</sup> restraint on the duplex. The hydrogens were then constrained using the SHAKE algorithm and the whole system relaxed by 2500 minimization steps. MD simulation was then initiated. While restraining the duplex with a 10 kcal mol<sup>-1</sup> Å<sup>-2</sup> force constant, the solvent environment was allowed to warm up to 298 K for 10 ps at constant volume using the Berendsen thermostat before the system was allowed to equilibrate unrestrained for 50 ps at 298 K and 1 atm (with time constants 1 ps and 2 ps, respectively). Finally, the dynamics of the system was simulated for 0.5 ns with time steps of 0.2 ps. The coordinates from the final 50 ps were used to produce an average structure of the final duplexes (Fig. 4).

## Acknowledgements

The Danish National Research Foundation, The Danish Research Agency and Møllerens Fond are thanked for financial support of the project, and Mrs Birthe Haack is thanked for technical assistance. We are grateful to the Danish Natural Science Research Council and to Carlsbergfondet for provision of the X-ray equipment in Odense, and to MAX-Lab, University of Lund, Sweden, for synchrotron access. Assistance at MAX-Lab was provided by Yngve Cerenius, Krister Larsson and Christer Svensson.

## References

- 1 C. J. Leumann, *Bioorg. Med. Chem.*, 2002, **10**, 841.
- 2 J. Kurreck, *Eur. J. Biochem.*, 2003, **270**, 1628.
- 3 J. Wengel, *Org. Biomol. Chem.*, 2004, **2**, 277.
- 4 B. Samori and G. Zuccheri, *Angew. Chem., Int. Ed.*, 2005, **44**, 1166.
- 5 N. C. Seeman and P. S. Lukeman, *Rep. Prog. Phys.*, 2005, **68**, 237.
- 6 A. Maddar, R. Ehrl and R. Strömberg, *ChemBioChem*, 2003, **4**, 1194.
- 7 K. Seio, T. Wada, K. Sakamoto, S. Yokoyama and M. Sekine, *J. Org. Chem.*, 1998, **63**, 1429.
- 8 W. Tongfei, M. Froeyen, G. Schepers, K. Mullens, J. Rozenski, R. Busson, A. Van Aerschot and P. Herdewijn, *Org. Lett.*, 2004, **6**, 51.
- 9 S. L. Pedersen and P. Nielsen, *Org. Biomol. Chem.*, 2005, **3**, 3570.
- 10 W. Tongfei, K. Nauwelaerts, A. Van Aerschot, M. Froeyen, E. Lescrier and P. Herdewijn, *J. Org. Chem.*, 2006, **71**, 5423.
- 11 M. S. Christensen, C. M. Madsen and P. Nielsen, *Org. Biomol. Chem.*, 2007, **5**, 1586.
- 12 P. Borsting, K. E. Nielsen and P. Nielsen, *Org. Biomol. Chem.*, 2005, **3**, 2183.
- 13 P. K. Sharma, B. H. Mikkelsen, M. S. Christensen, K. E. Nielsen, C. Kirchhoff, S. L. Pedersen, A. M. Sørensen, K. Østergaard, M. Petersen and P. Nielsen, *Org. Biomol. Chem.*, 2006, **4**, 2433.
- 14 P. Nielsen, L. H. Dreieø and J. Wengel, *Bioorg. Med. Chem.*, 1995, **3**, 19.
- 15 O. L. Acevedo and R. S. Andrews, *Tetrahedron Lett.*, 1996, **37**, 3931.
- 16 A. Holy, *Collect. Czech. Chem. Commun.*, 1975, **40**, 187.
- 17 L. Zhang, A. Peritz and E. Meggers, *J. Am. Chem. Soc.*, 2005, **127**, 4174.
- 18 L. Zhang, A. E. Peritz, P. J. Carroll and E. Meggers, *Synthesis*, 2006, **4**, 645.
- 19 K.-U. Schöning, P. Scholz, S. Guntha, X. Wu, R. Krishnamurthy and A. Eschenmoser, *Science*, 2000, **290**, 1347.
- 20 O. Mitsunobu, *Synthesis*, 1981, 1.
- 21 M. Frieden, M. Giraud, C. B. Reese and Q. Song, *J. Chem. Soc., Perkin Trans. 1*, 1998, **290**, 2827.
- 22 A.-I. Hernández, J. Balzarini, A. Karlsson, M.-J. Camarasa and M.-J. Pérez-Pérez, *J. Med. Chem.*, 2002, **45**, 4254.
- 23 J. J. Fox and N. C. Miller, *J. Org. Chem.*, 1963, **28**, 936.
- 24 M. Beier and W. Pfeleiderer, *Helv. Chim. Acta*, 1999, **82**, 879.
- 25 D. Zhou, I. M. Lagoja, J. Rozenski, R. Busson, A. Van Aerschot and P. Herdewijn, *ChemBioChem*, 2005, **6**, 2298.
- 26 D. G. Gorenstein, *Phosphorus-31 NMR: Principles and Applications*, Academic Press, New York, 1984.
- 27 C. J. Wilds, Z. Wawrzak, R. Krishnamurthy and A. Eschenmoser, *J. Am. Chem. Soc.*, 2002, **124**, 13716.
- 28 R.-I. Ma, N. R. Kallenbach, R. D. Sheardy, M. L. Petrillo and N. C. Seeman, *Nucleic Acids Res.*, 1986, **14**, 9745.
- 29 N. B. Leontis, W. Kwok and J. S. Newman, *Nucleic Acids Res.*, 1991, **19**, 759.
- 30 B. Liu, N. B. Leontis and N. C. Seeman, *Nanobiology*, 1994, **3**, 177.
- 31 C. Svensson, *TWINSOLVE*, University of Lund, Sweden, 2004.
- 32 G. M. Sheldrick, *SHELXTL*, Bruker AXS, Madison, Wisconsin, USA, 2000.
- 33 D. A. Case, D. A. Pearlman, J. W. Caldwell, T. E. Cheatham III, J. Wang, W. S. Ross, C. L. Simmerling, T. A. Darden, K. M. Merz, R. V. Stanton, A. L. Cheng, J. J. Vincent, M. Crowley, V. Tsui, H. Gohlke, R. J. Radmer, Y. Duan, J. Pitera, I. Massova, G. L. Seibel, U. C. Singh, P. K. Weiner and P. A. Kollman, *AMBER7*, University of California, San Francisco, 2002.
- 34 M. W. Schmidt, K. K. Baldridge, J. A. Boatz, S. T. Elbert, M. S. Gordon, J. H. Jensen, S. Koseki, N. Matsunaga, K. A. Nguyen, S. Su, T. L. Windus, M. Dupuis and J. A. Montgomery, Jr., *J. Comput. Chem.*, 1993, **14**, 1347.